Conf-941144--60

PNL-SA-25670

EFFECTS OF HELIUM PRE-IMPLANTATION ON THE MICROSTRUCTURE AND MECHANICAL PROPERTIES OF IRRADIATED 316 STAINLESS STEEL

M. L. Hamilton
M. B. Toloczko[a]
G. R. Tedeski[a]
G. E. Lucas[a]
G. R. Odette[a]
R. E. Stoller[b]

November 1994

Presented at the
Symposium on Microstructure of Irradiated Materials
Conference
November 28 - December 2, 1995
Boston, Massachusetts

Prepared for
the U.S. Department of Energy
under Contract DE-AC06-76RLO 1830

Pacific Northwest Laboratory
Richland, Washington 99352

(a) University of California, Santa Barbara, California
(b) Oak Ridge National Laboratory, Oak Ridge, Tennessee

EFFECTS OF HELIUM PRE-IMPLANTATION ON THE MICROSTRUCTURE AND MECHANICAL PROPERTIES OF IRRADIATED 316 STAINLESS STEEL

Mychailo B. Toloczko*, Gregg R. Tedeski*, Glenn E. Lucas*, G. Robert Odette*, Roger E. Stoller**, and Margaret L. Hamilton***
*Department of Chemical and Nuclear Engineering, University of California, Santa Barbara, CA 93106
**Oak Ridge National Laboratory, P.O. Box 2008, Oak Ridge, TN 37831-6151
***Pacific Northwest Laboratory, P.O. Box 999, Richland, WA 99352

ABSTRACT

Transmission electron microscopy (TEM) specimens of a First Core heat of 316 stainless steel, in both the solution annealed and 20% cold worked condition, were irradiated to 46 dpa at 420°C, to 49 dpa at 520°C, and to 34 dpa at 600°C in FFTF/MOTA. Prior to irradiation, about half of the specimens were pre-implanted with approximately 100 appm of helium, and of these, several of the solution annealed and pre-implanted specimens were aged at 800°C for 2hr. Post-irradiation density measurements showed little difference in density between the unimplanted alloys and their helium implanted counterparts. Microstructural observations on specimens irradiated at 420°C and 520°C showed relatively minor differences in defect distributions between the unimplanted and the helium implanted materials; in all cases the defect sizes and number densities were consistent with data in the literature. Where possible, irradiation hardening of the alloys was experimentally evaluated by microhardness and shear punch; experimentally obtained values were compared to values calculated using a computer model based on barrier hardening and the microstructural data. All methods indicated relatively small effects of helium implantation, and both measured and calculated values were in agreement with the range of values reported in the literature.

INTRODUCTION

Austenitic stainless steels are partially limited for use in fusion reactors by the potential for transmutant helium to affect both the swelling and mechanical properties, and a considerable body of literature has been amassed to investigate this [1-9]. Reported here are the data obtained to date on solution annealed and cold worked austenitic stainless steels that were successfully irradiated in an experiment devised to examine the effects of pre-implanted helium on the microstructural evolution and mechanical properties of both austenitic and ferritic stainless steels.

EXPERIMENT

TEM specimens for irradiation were fabricated from 316 stainless steel (First Core heat 81585) in two material conditions: 1) solution annealed (SA) at 1050°C for 0.5 hours and 2) 20% cold worked (CW). Sheet coupons were exposed to a 6 μA defocused beam of 40 MeV alpha particles at the University of California Davis cyclotron facility. Uniform helium concentration through the coupons was achieved by varying the angle of the coupon face with the beam and the time spent at that angle. From records of total exposure of the coupons to the α-beam, the average concentration of helium in the implanted coupons was calculated to be 100 appm. (Cross sectional nonuniformity of the beam intensity resulted in a few specimens having much greater than or much less than the 100 appm average.) Approximately half of the implanted SA specimens were then

aged at 800°C for 2hr in helium-filled quartz capsules. Specimens were irradiated in FFTF/MOTA to doses of 46 dpa at 420°C, 49 dpa at 520°C, and 34 dpa at 600°C. Following irradiation, specimens were subjected to densitometry, transmission electron microscopy (TEM), and shear punch testing at PNL. Microhardness testing and additional TEM were performed at UCSB. Yield stresses were determined from both microhardness and shear punch measurements using linear correlations established from microhardness, shear punch, and tensile tests on unirradiated 316 SS specimens having a wide range of strengths. Details on the analysis procedures can be found elsewhere [10-13]. The material designation and specimen matrix is shown in Table 1.

Condition (420, 520, 600°C)	Densitometry	TEM	Microhardness	Shear Punch
SA	y, y, y	y, y, n	y, y, y	n, n, y
SA.He	y, n, y	y, n, n	y, n, y	y, n, n
SA.He.age	y, y, y	y, y, n	y, y, y	y, n, n
CW	y, y, y	y, n, n	y, y, y	y, y, y
CW.He	y, y, y	y, n, n	y, y, y	y, y, y

Table 1. Types of examination performed on each specimen type irradiated at 420°C, 520°C, and 600°C. y = yes; n = no; corresponds to each of the three irradiation temperatures.

RESULTS/DISCUSSION

Swelling and Microstructural Evolution

The swelling results determined from densitometry and microscopy are plotted in Figure 1. The cavity-based values are consistently larger than the densitometry-based values by approximately the same amount for both the SA and the CW material. Such discrepancies between the two techniques have been reported in other studies [2], and have been attributed, in part, to the effect of precipitation on density and to the magnitude in the uncertainty in the densitometry technique when the total swelling is small. The effect of helium implantation on the response of SA and CW material is mixed. In the SA and CW material at 420°C, the densitometry-based values suggest a slight increase in swelling with the addition of helium. Swelling calculated from microscopy at the same temperature shows the same small increase in swelling with helium in the SA material, but the CW material shows no helium-implantation effect. In the SA and CW material at 520°C, density and microscopy based swelling measurements suggest that helium pre-implantation may suppress swelling. The mixed effect at 600°C is complicated by large variations in helium pre-implanation as shown in Figure 1.

The microstructural features of the irradiated specimens observed in the TEM are summarized in Tables 2 and 3. The observed irradiated microstructures were broadly consistent with changes reported in austenitic stainless steels: the major microstructural features consisted of network dislocations, faulted loops, cavities, and precipitates [2,3,8,12,14-19]. At 420°C, network dislocation densities, ρ_n, increase with helium in the SA, while they decrease in the CW. At 520°C, the network dislocation density decreases. The faulted loop dislocation densities, ρ_L, follow approximately the same trend, but their values are about 25% of the network dislocation densities. In all cases, the differences in the dislocation densities are within experimental error. A strong helium effect is not obvious. For the SA, the dislocation densities drop with an increase in irradiation temperature. For SA and CW at 420°C and 520°C, faulted loop sizes, d_L, show only

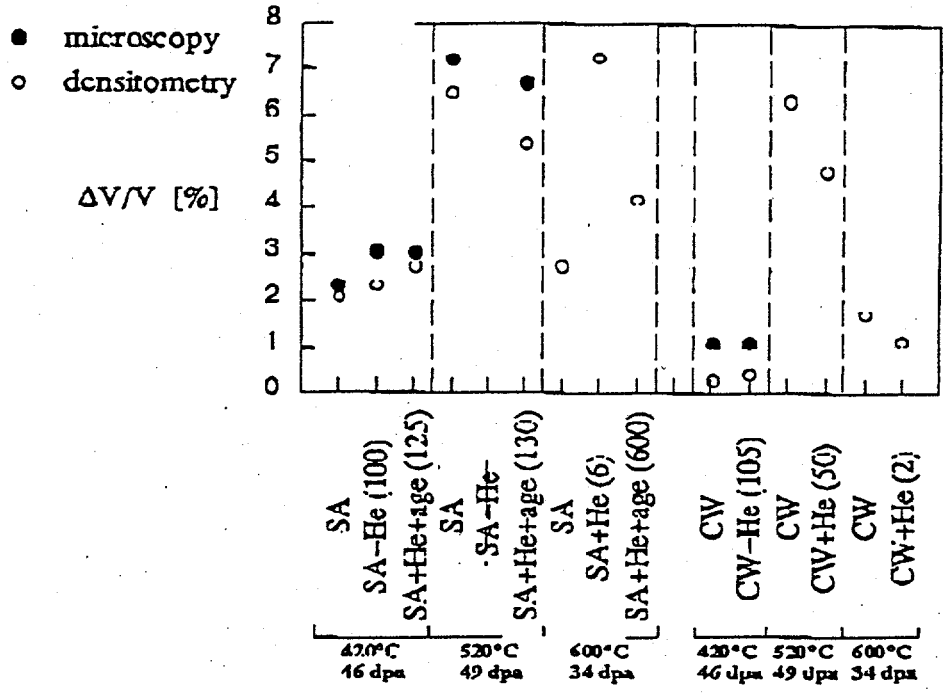

Figure 1. Swelling versus temperature as calculated from densitometry and microscopy. Helium content in appm is shown in parenthesis.

minor size differences for the different pre-implanation conditions, however loop number densities, N_l, show a moderate decrease with helium for the SA and CW at 420°C. Cavities sizes, d_v, display trends similar to d_l at 420°C, however at 520°C, the cavity size in the SA_He_age is about 10 nm larger than in the SA. At 420°C in the SA, the cavity number density, N_v, increases with helium, while it is constant with helium in the CW. At 520°C in the SA, where there was a significant increase in cavity size with helium, the cavity number density shows a corresponding decrease. Precipitates show nearly the same trends as cavities except at 520°C, the precipitate number density, N_p, does not show the same corresponding decrease that was seen in the cavity number density at that temperature. Additionally, N_p decreases with helium in the CW at 420°C.

Material	*He cont [appm]*	*dpa*	*Temp [°C]*	ρ_n $[10^{10}\ cm^{-2}]$	d_L *[nm]*	N_L $[10^{15} cm^{-3}]$	ρ_L $[10^{15} cm^{-2}]$
SA	0	49	420	9.8	25.9	2.34	1.9
SA_He	77	49	420	13.3	30.4	2.20	2.1
SA_He_age	121	49	420	15.2	27.0	1.50	1.3
SA	0	46	520	9.0	54.6	0.35	0.6
SA_He_age	124	46	520	7.9	49.2	0.39	0.6
CW	0	49	420	19.4	29.9	6.18	5.8
CW_He	101	49	420	15.9	29.2	4.80	4.4

Table 2. Dislocation densities and faulted loop sizes and number densities at about 50 dpa.

Material	He cont [appm]	dpa	Temp [°C]	d_v [nm]	N_v [10^{15} cm^{-3}]	d_p [nm]	N_p [10^{15} cm^{-3}]
SA	0	49	420	26.0	2.06	24.3	1.62
SA.He	77	49	420	26.6	2.62	25.8	2.35
SA.He.age	121	49	420	27.0	2.45	24.8	2.29
SA	0	46	520	62.3	0.38	44.6	0.30
SA.He.age	124	46	520	72.0	0.25	58.7	0.34
CW	0	49	420	17.6	3.18	18.4	2.86
CW.He	101	49	420	17.2	3.18	17.7	2.33

Table 3. Cavity and precipitate sizes and number densities at approximately 50 dpa.

Conclusions about the effect of helium on these microstructural defects can be summarized as follows: 1) If there is an effect, it is complex; 2) The minor helium effect appeared to be dependent on irradiation temperature and prior thermomechanical treatment and varies with defect type; 3) In most cases, the differences exhibited between unimplanted and implanted material are within the experimental error. Similar conclusions have been previously reported [6,8].

Mechanical Properties

The correlated yield stresses determined from microhardness and shear punch tests are shown in figure 2. The lines (solid for CW and dashed for SA) are drawn from the unirradiated yield stress to the average of the irradiated values simply to guide the eye, however they are representative of the trends seen in the literature where the yield stress change saturates by about 10-20 dpa in this irradiation temperature regime [17-25]. Following trends reported in the literature, the yield

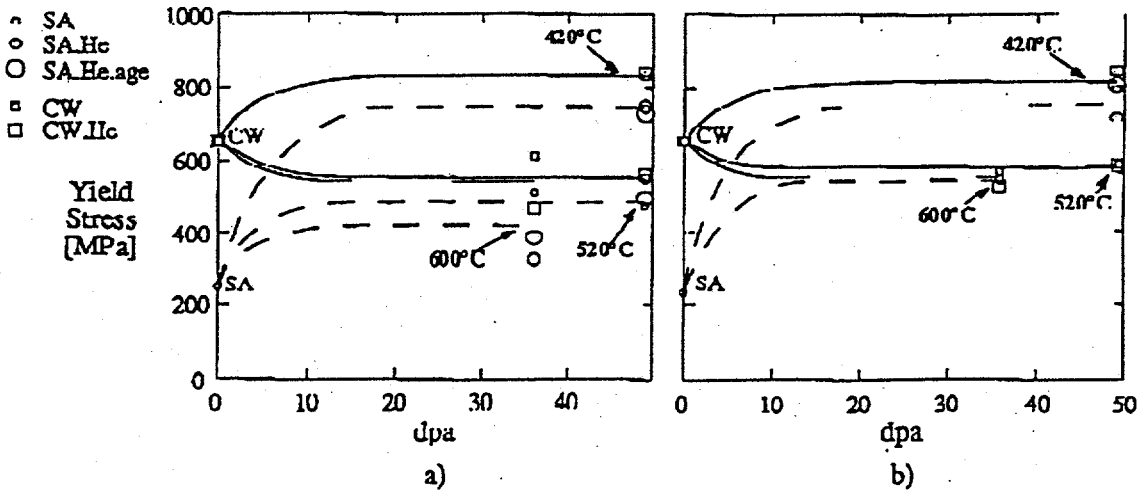

Figure. 2 Dose dependence of uniaxial yield stress determined from a) microhardness and b) shear punch tests.

stress increases at all temperatures for the SA, and the change decreases with increasing temperature. The CW material increases in yield stress at 420°C but decreases at 520 and 600°C. There does not appear to be a strong effect of helium on yield stress change in either material, except possibly on the microhardness tests at 600°C and 34 dpa; however, as mentioned previously, there are large differences in helium contents of these specimens, and the yield stress variation seen in the microhardness tests of the CW material at 600°C are not seen in the shear punch tests. At each temperature, the yield strengths of SA and CW materials show significant convergence.

The microstructural defect data were used to estimate the yield stress using a computer simulation based on the barrier hardening model. The total yield strength of the irradiated material, σ_y, was assumed to have the form

$$\sigma_y = \sigma_o + \sigma_{lr} + \Delta\sigma_{sr}$$

where σ_o is the yield stress of unirradiated SA material (taken to be 225 MPa), σ_{lr} is the long range stress field due to network dislocations (taken to be proportional to $\sqrt{\rho_n}$), and $\Delta\sigma_{sr}$ is the increase in yield stress due to short range obstacles. The value of $\Delta\sigma_{sr}$ was determined by modelling the motion of a dislocation through a two-dimensional obstacle field similar to that of Foreman and Makin [26]. Critical angles, θ_c, for dislocation release from obstacles were determined from assigned barrier strengths using the relation $\alpha = \cos(\theta_c/2)$. Short range obstacles were taken to be loops, precipitates, and cavities with barrier strengths 0.3, 0.6, and 1.0 respectively [15]. Planar number densities of each defect were determined from the square root of the product of measured volume number densities and defect sizes, but the defects were assigned random positions in the glide plane, and the defects were treated as point obstacles. The resulting predictions are compared to measured values of yield stress determined from both shear punch and microhardness measurements in Figure 3. The model predictions track the experimentally-based values reasonably well, however, contrary to mechanical properties tests, the notably different CW and SA microstructures combined with the simulations did not predict a yield strength difference between SA and CW materials. The simulations suggest the major contributions to hardening

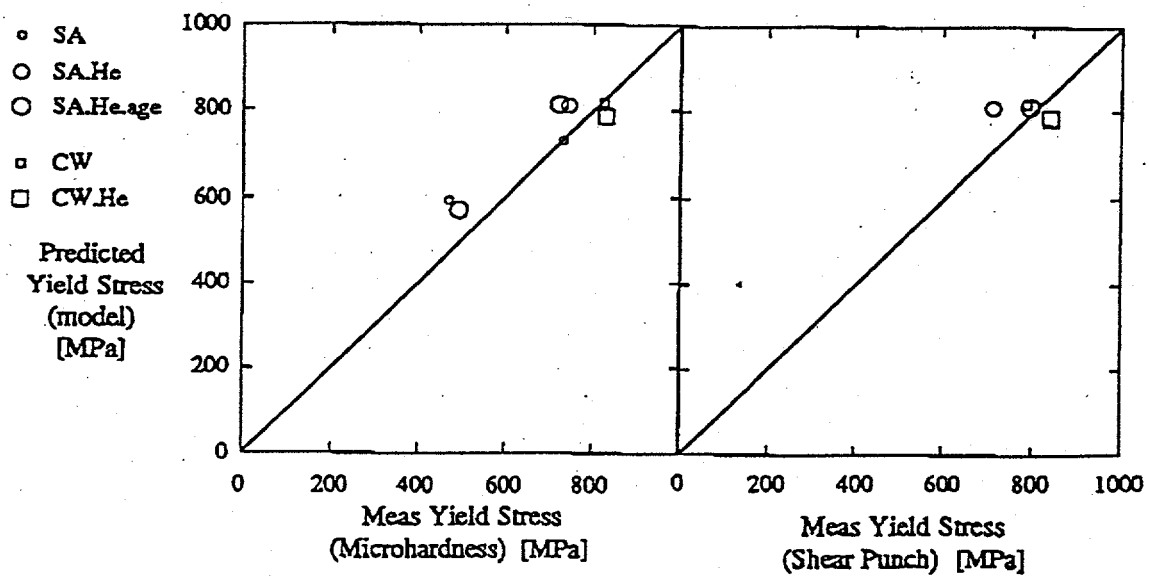

Figure 3. Comparison of the uniaxial yield stress predicted from the barrier hardening model with values determined from microhardness and shear punch tests.

come from the network dislocations and voids, with voids contributing about twice as much as dislocations. Bubbles, which were not included in this hardening analysis, also act as short range barriers. Based on bubble densities from previous studies of helium pre-implantation of austenitics [3], their contribution could be up to 30 MPa of hardening. Results from this and other experiments show that helium's effect on mechanical properties is manifested in its observable changes to the microstructure [24,25].

SUMMARY/CONCLUSIONS

A First Core heat of 316 stainless steel in both the CW and SA condition was irradiated to ~50 dpa at 420°C and 520°C and to 34 dpa at 600°C. Some specimens were cold pre-implanted with helium (~100 appm) or cold pre-implanted with helium and aged (SA only) prior to irradiation. With the exception of the implanted SA specimen (6 appm of pre-implanted helium) irradiated at 600°C, the observed swelling as a function of temperature achieved a maximum at 520°C with little observed effect of helium on either the cavity swelling or the density. At 420°C and 520°C where irradiation-induced microstructural defects were characterized, network dislocation densities and faulted loop, cavity, and precipitate sizes and number densities were consistent with trends reported in the literature; again, a strong effect of helium pre-implantation on the microstructure was not observed. Yield stress changes as determined by microhardness, shear punch techniques, and barrier hardening models show agreement among themselves and with the data trends from the literature. The barrier hardening analysis suggests that the major hardening comes from network dislocations and voids, reconciling the apparent absence of a helium effect on yield stress.

ACKNOWLEDGEMENTS

This work was funded by the Department of Energy, Office of Fusion Energy under grants DE FG03-87ER-52143 and DE-AC06-76RLO-1830. Support for R.E. Stoller provided in part by Division of Materials Science, U.S. DOE under contract DE-AC05-84OR-21400.

REFERENCES

1. Odette, G.R., Maziasz, P.J., and Spitznagel J.A., J. Nucl. Mater., **103 & 104**, pp. 1289-1304 (1981).
2. Maziasz, P.J., Effect of Helium Content on Microstructural Development in Type 316 SS Under Neutron Irradiation, ORNL-6121 (1985).
3. Stoller, R.E., J. Nucl. Mater., **174**, pp 289-310 (1990).
4. Scott, J.L., et. al., ADIP Semiannual Progress Report, DOE/ER-0045/14, US. Department of Energy, March 31, 1985.
5. Mansur, L.K., Rowcliffe, A.F., Grossbeck, M.L., and Stoller, R.E., J. Nucl. Mater., **139**, pp. 228-236 (1986).
6. Stubbins, J.F., and Garner, F.A., J. Nucl. Mater., **179-181**, pp. 523-525 (1991); **191-194**, pp. 1300-1304 (1992).
7. Sekimura, N., Garner, F.A., and Griffin, R.D., J. Nucl. Mater. **191-194**, pp. 1234-1238 (1992).
8. Brager, H.R., and Garner, F.A., J. Nucl. Mater., **117**, pp. 159-176 (1983).
9. Garner, F.A., and Greenwood, L.R., Mat. Trans. JIM, **34**, pp. 985-998 (1993)
10. Lucas, G.E., Mader, E., and Odette, G.R., "Effects of Metallurgical Variable and Irradiation Conditions on the Kinetics of Post Irradiation Annealing of Pressure Vessel Steels",

Proceedings of Fourth International Symposium on Environmental Degradation of Materials in Nuclear Power Systems - Water Reactors, NACE-TMS/AIME-ANS, August 6-10 1989, Jeckyll Island, GA (1990).
11. Lucas, G.E., Odette, G.R., and Sheckard, J.W., ASTM **STP 888**, W.R. Corwin and G.E. Lucas, Eds., American Society for Testing and Materials, Philadelphia, pp. 112-140 (1986).
12. Odette, G.R., Lucas, G.E., Stoller, R.E., and Phythian, W., "On the Effect of Flux and Composition on Irradiation Hardening at 60°C", ASTM **STP 1270**, D.S. Gelles, R.K. Nanstad, A.S. Kumar, and E.A. Little, Eds., American Society for Testing and Materials, Phil., (1994).
13. Toloczko, M.B., Lucas, G.E., Odette, G.R., Stoller, R.E., and Hamilton, M.L., "Effects of Helium Pre-Implantation on the Microstructure and Mechanical Properties of Irradiated 316 Stainless Steel", ASTM **STP 1270**, D.S. Gelles, R.K. Nanstad, A.S. Kumar, and E.A. Little, Eds., American Society for Testing and Materials, Philadelphia, (1994).
14. Stoller, R.E., and Odette, G.R., J. Nucl. Mater., **154**, pp. 286-304, (1988).
15. Lucas, G.E., J. Nucl. Mater., **206**, pp. 287-305 (1993).
16. Zinkle, S.J., Maziasz, P.J., and Stoller, R.E., J. Nucl. Mater., **206**, pp. 266-286 (1993).
17. Garner, F.A., and Gelles D.S., ASTM **STP 1046**, N.H. Packan, R.E. Stoller, and A.S. Kumar, Eds., American Society for Testing and Materials, Philadelphia, pp. 673-683 (1990).
18. Maziasz, P.J., and Grossbeck, M.L., J. Nucl. Mater., **103 & 104**, pp. 987-992 (1981).
19. Katoh, Y., Kohno, Y., and Kohyama, A., J. Nucl. Mater, **212-215**, pp. 464-470 (1994)
20. Johnson, G.D., Garner, F.A., Brager, H.R., and Fish, R.L., ASTM **STP 725**, D. Kramer, H.R. Brager, and J.S. Perrin, Eds., American Society for Testing and Materials, Philadelphia, pp. 393-412 (1981).
21. Holmes, J.J., and Straalsund, J.L., Proceedings of International Conference on Radiation Effects in Breeder Reactor Structural Materials, The Metallurgical Society of AIME, Scottsdale, New York, pp. 53-63 (1977).
22. Bagley, K.Q., Barnaby, J.W., and Fraser, A.S., Proceedings of Conference on Irradiation Embrittlement and Creep of Fuel Cladding and Core Components, British Nuclear Energy Society, London, pp. 143-153 (1972).
23. Garner, F.A., J. Nucl. Mater., **206**, pp. 230-248 (1993).
24. Hamilton, M.L., Okada, A., and Garner, F.A., J. Nucl. Mater., **179-181**, pp. 558-562 (1991).
25. Garner, F.A., Hamilton, M.L., Greenwood, L.R., Stubbins, J.F., and Oliver, B.M., ASTM **STP 1175**, pp. 921-939 (1992).
26. Foreman, A.J.E., and Makin, A.J., Can. J. Phys., **45**, pp. 511 (1967).